Polymer 55 (2014) 3093–3099

Contents lists available at ScienceDirect

Polymer

journal homepage: www.elsevier.com/locate/polymer

Thieno[3,2-b]thiophene as π-bridge at different acceptor systems for electrochromic applications

Sinem Toksabay [a], Serife O. Hacioglu [a], Naime A. Unlu [a], Ali Cirpan [a, b, c, d], Levent Toppare [a, b, c, e, *]

[a] Department of Chemistry, Middle East Technical University, 06800 Ankara, Turkey
[b] Department of Polymer Science and Technology, Middle East Technical University, 06800 Ankara, Turkey
[c] The Center for Solar Energy Research and Application (GÜNAM), Middle East Technical University, 06800 Ankara, Turkey
[d] Department of Micro and Nanotechnology, Middle East Technical University, Ankara 06800, Turkey
[e] Department of Biotechnology, Middle East Technical University, 06800 Ankara, Turkey

ARTICLE INFO

Article history:
Received 7 April 2014
Received in revised form
8 May 2014
Accepted 11 May 2014
Available online 22 May 2014

Keywords:
Conjugated polymers
Electrochromism
thieno[3,2-b]thiophene

ABSTRACT

Benzoselenadiazole, quinoxaline and thieno[3,2-b]thiophene are the units preferred in conducting polymers due to their electrochemical properties. There are no reports in the literature on polymers containing both moieties. In this study, novel benzoselenadiazole, quinoxaline and thieno[3,2-b]thiophene based monomers; 4-(3a,6a-dihydrothieno[3,2-b]thiophen-2-yl)-7-(thieno[3,2-b]thiophenyl) benzo[c][1,2,5]selenadiazole **(BSeTT)** and 2,3-bis(3,4-bis(decyloxy)phenyl)-5,8-dibromo-2,3-dihydroquinoxaline **(QTT)** were synthesized via Stille Coupling and polymerized electrochemically. These polymers were characterized in terms of their spectroelectrochemical and electrochemical properties by cyclic voltammetry and UV–Vis–NIR spectroscopy. Spectroelectrochemistry analysis of **PBSeTT** revealed an electronic transition at 525 nm corresponding to π–π* transition with a band gap of 0.93 eV whereas **PQTT** revealed electronic transitions at 440 and 600 nm corresponding to π–π* transitions with a band gap of 1.30 eV. Electrochromic investigations showed that **PBSeTT** has gray color **PQTT** switching between green and gray. Switching time of the polymers was evaluated by a kinetic study upon measuring the percent transmittance (%T) at the maximum contrast point.

1. Introduction

A new age had been started in macromolecular science with the invention of conducting polymers [1] and they have gained considerable attention due to the their advantages of low cost, high weight, easy fabrication and compability with flexible substrates [2–4]. It was found that they can be used in many fields, such as organic light emitting diodes [5], electrochromic materials [6], organic solar cells [7], organic field effect transistors [8] and sensors [9]. Since band gap of the polymer plays an important role to accomplish desired applications [10], there are many approaches for manipulating it. However, the donor–acceptor phenomenon, which provide the band gap alternation due to the electron rich and electron poor building blocks in the polymer main chain, is one of the most exploited technique for designing organic conducting polymers [11]. Through regulating the contribution of intramolecular charge transfer (ICT), the absorption spectra and energy levels of D-A type polymers can be tuned [12]. Based on this, donor–acceptor conjugated polymers have been extensively used as a low band-gap donor materials in achieving high performance polymer solar cells (PSCs) [13,14]. Therefore, many different types of low band gap polymers have been synthesized and developed for this purpose. 1,2,3-Benzotriazole [15], diketopyrrolopyrrole [16], thieno [3,4-b] pyrazine [17], 2,1,3-benzothiadiazole [18], are mostly preferred acceptor type units to design donor–acceptor type low band gap molecules. Due to the their good electron-withdrawing properties benzothiadiazole derivatives are used to generate low band gap molecules for photovoltaic and electroluminescent devices especially [19]. Owing to the good electron-withdrawing feature, benzoselenadiazole is one of the mostly used unit in D-A type low band gap polymer [20]. Benzoselenadiazole (BSe) is generated by replacing the sulfur atom in the benzothiadiazole (BT) unit with selenium. Polymers containing benzoselenadiazole (BSe) building block have lower HOMO energy level than those having benzothiadiazole (BT) unit due to selenium's larger size and

* Corresponding author. Department of Chemistry, Middle East Technical University, 06800 Ankara, Turkey.
E-mail address: toppare@metu.edu.tr (L. Toppare).

http://dx.doi.org/10.1016/j.polymer.2014.05.029
0032-3861/

stronger electron affinity [21]. In addition to this, selenium comprising polymers have red shift in the absorption spectrum compared to sulfur containing polymers [22–24]. The selenophene unit could also enhance inter-chain interactions between polymer chains via strong Se–Se interactions [25].

Also, among an extensive range of acceptor units, quinoxaline units (Qx) have been demonstrated to be an admirable building block for synthesis of low band gap conjugated polymers due to the their electron withdrawing feature of two imine nitrogens in the Qx. In terms of providing the utility of introducing substituents easily on the 2 and 3 positions of itself, the Qx unit has a great structure for controlling the electronic structure of the ending polymers [26].

On the other hand, photoactive semiconductor materials using in PSCs are recently developed to enhance their performance. For this purpose, the incorporation of π-conjugated, rigidly fused thiophene rings are used in a conjugated polymer main chain, since fused thiophene rings can make the molecular backbone more rigid and coplanar [27]. In addition, materials having fused thiophene rings remarkably attractive owing to the their great optoelectronic properties consist of aromatic coupled structures with extending π-conjugated length, facilitating the achievement of closely packed conjugated backbones and consequently more effective charge intermolecular hopping and transport [28]. Among large number of fused-ring structures, thieno[3,2-b]thiophene derivatives with fused two thiophene rings have attracted scientific interest due to the their symmetrical, planar structure and their potential to provide high charge carrier mobility due to its planar structure enhancing π-stacking ability of resulting polymer [29]. Also, discussion on the effect of thieno[3,2-b]thiophene on the properties of polymers containing Bse and Qx acceptors lacks in literature. With this aim, we designed and synthesized polymers consisting of BSe, Qx and thieno[3,2-b]thiophene moieties.

2. Experimental section

2.1. General

All reagents were obtained from commercial sources and used without further purification unless otherwise mentioned. THF was dried over sodium and benzophenone. 3,6-Dibromobenzene-1,2-diamine [30] tributyl(thieno[3,2-b]thiophen-2-yl)stannane [31] 4,7-dibromobenzo[c][1,2,5]selenadiazole [32] and 2,3-bis(3,4-bis(decyloxy)phenyl)-5,8-dibromo-2,3-dihydroquinoxaline [33] were synthesized according to previously published procedures. ^{1}H NMR and ^{13}C NMR spectra were recorded in $CDCl_3$ on Bruker Spectrospin Avance DPX-400 Spectrometer with TMS as the internal reference. Electropolymerization was performed in a three electrode cell consisting of an Indium Tin Oxide doped glass slide (ITO) as the working electrode, platinum wire as the counter electrode, and Ag wire as the pseudo reference electrode under ambient conditions using a Gamry potentiostat. Before each measurement, argon gas was purged into the dichloromethane solution for 5 min. The reference electrode was subsequently calibrated to Fc/Fc^+ and the band energies were calculated relative to the vacuum level taking the value of SHE as −4.75 eV [23]. Spectroelectrochemical studies of polymers were carried out using Varian Cary 5000 UV–Vis spectrophotometer.

2.1.1. Synthesis of 4,7-di(thieno[3,2-b]thiophen-2-yl)benzo[c][1,2,5]selenadiazole

4,7-Dibromobenzo[c][1,2,5]selenadiazole (200 mg, 0.6 mmol) and tributyl[thieno[3,2-b]thiophen-2-yl]stannane (515.2 mg, 1.2 mmol) were dissolved in dry THF (100 mL). The mixture was degased with argon for 30 min and $PdCl_2(PPh_3)_2$ (50 mg, 0.071 mmol) was added at room temperature under inert atmosphere. The mixture was stirred at 100 °C under argon atmosphere for 15 h, cooled and concentrated on the rotary evaporator. The residue was subjected to column chromatography to afford dark purple solid (silica gel, $CHCl_3$:hexane, 1:1).

^{1}H NMR (400 MHz, $CDCl_3$, δ):8.33 (s,2H), 7.73 (s,2H), 7.38(d, J = 5.2 Hz, 2H), 7.23 (d, J = 5.3 Hz, 2H).

^{13}C NMR (100 MHz, $CDCl_3$, δ):162.6, 146.7, 146.1, 138.4, 134.9, 131.2, 131.1, 130.9, 127.4, 127.3, 118.4.

2.1.2. Synthesis of 2,3-bis(3,4-bis(decyloxy)phenyl)-5,8-di(thieno[3,2-b]thiophen-2-yl)-2,3-dihydroquinoxaline

2,3-Bis[3,4-bis[decyloxy]phenyl]-5,8-dibromoquinoxaline (200 mg, 0.2 mmol) and tributyl[thieno[3,2-b]thiophen-2-yl]stannane (171.7 mg, 0.4 mmol) were dissolved in dry THF (100 mL). The mixture was degased with argon for 30 min and $Pd(PPh_3)_2Cl_2$ (50 mg, 0.071 mmol) was added at room temperature under an inert atmosphere. The mixture was stirred at 100 °C under argon atmosphere for 15 h, cooled and concentrated on the rotary evaporator. The residue was subjected to column chromatography to afford an orange solid (silica gel, $CHCl_3$:hexane 1:1).

^{1}H NMR (400 MHz, $CDCl_3$, δ):8.06 (d, J = 6.9 Hz, 2H), 7.47(s, 2H), 7.35 (d, J = 5.2 Hz, 2H), 7.22 (d, J = 5.2 Hz, 2H), 7.16(s, 2H), 6.77 (d, J = 8.4 Hz, 2H), 3.97 (t, J = 6.6 Hz, 8H), 3.92(d, J = 6.6 Hz, 8H), 1.77(m, J = 7.9 Hz, 30H), 1.44(m, J = 7.6 Hz, 8H), 0.82(t, J = 4.4 Hz, 30H).

^{13}C NMR (100 MHz, $CDCl_3$, δ):163.6, 154.5, 149.2, 141.5, 132.5, 126.5, 122.5, 118.5, 117.8, 114.7, 111.8, 68.22, 68.15, 30.92, 29.88, 28.78, 28.71, 28.65, 28.60, 28.47, 28.45, 28.39, 28.35, 28.28, 25.16, 25.07, 21.68, 13.09.

3. Results and discussion

3.1. Synthesis

Synthetic route of monomers was presented in Scheme 1. Previously published procedure was utilized for the syntheses of 4,7-dibromobenzo[c][1,2,5]selenadiazole [32], 2,3-bis[3,4-bis[decyloxy]phenyl]-5,8-dibromoquinoxaline [33], tributyl[thieno[3,2-b]thiophen-2-yl]stannane [31]. Syntheses of **QTT** and **BSeTT** were performed via Stille coupling in the presence of $Pd(PPh_3)_2Cl_2$ and THF.

3.2. Electrochemical properties

To get a deeper perspective on the electrochemical and spectroelectrochemical properties of conjugated polymers, different methods have been conducted as a further characterization and results are summarized in this section. Cyclic voltammetry (CV) studies were performed both for electrochemical polymerization of monomers and investigation of the redox properties of the electrochemically synthesized polymers. The system consists of a potentiostat and a cell bearing indium tin oxide (ITO) coated glass plate as working electrode, platinum wire as counter and Ag wire pseudo reference electrodes.

Both **BSeTT** and **QTT** were polymerized potentiodynamically on ITO coated glass slide. While electrochemical polymerization of **BSeTT** was performed in a 0.1 M $NaClO_4/LiClO_4$ (1:1)/ACN:DCM (acetonitrile: dichloromethane) (95:5) solution, the system for electropolymerization of **QTT** as $NaClO_4/LiClO_4$ (1:1)/ACN:DCM (1:1) is preferred due to the low solubility of this derivative. The cyclic voltammograms for electrochemical polymerizations scanned between 0 V/1.6 V and between 0 V/1.1 V at a scan rate of 100 mV/s, respectively are reported Fig. 1.

In the first cycle of CV irreversible monomer oxidation peaks were recorded at 1.39 V and at 0.83 V for **BSeTT** and **QTT**, respectively.

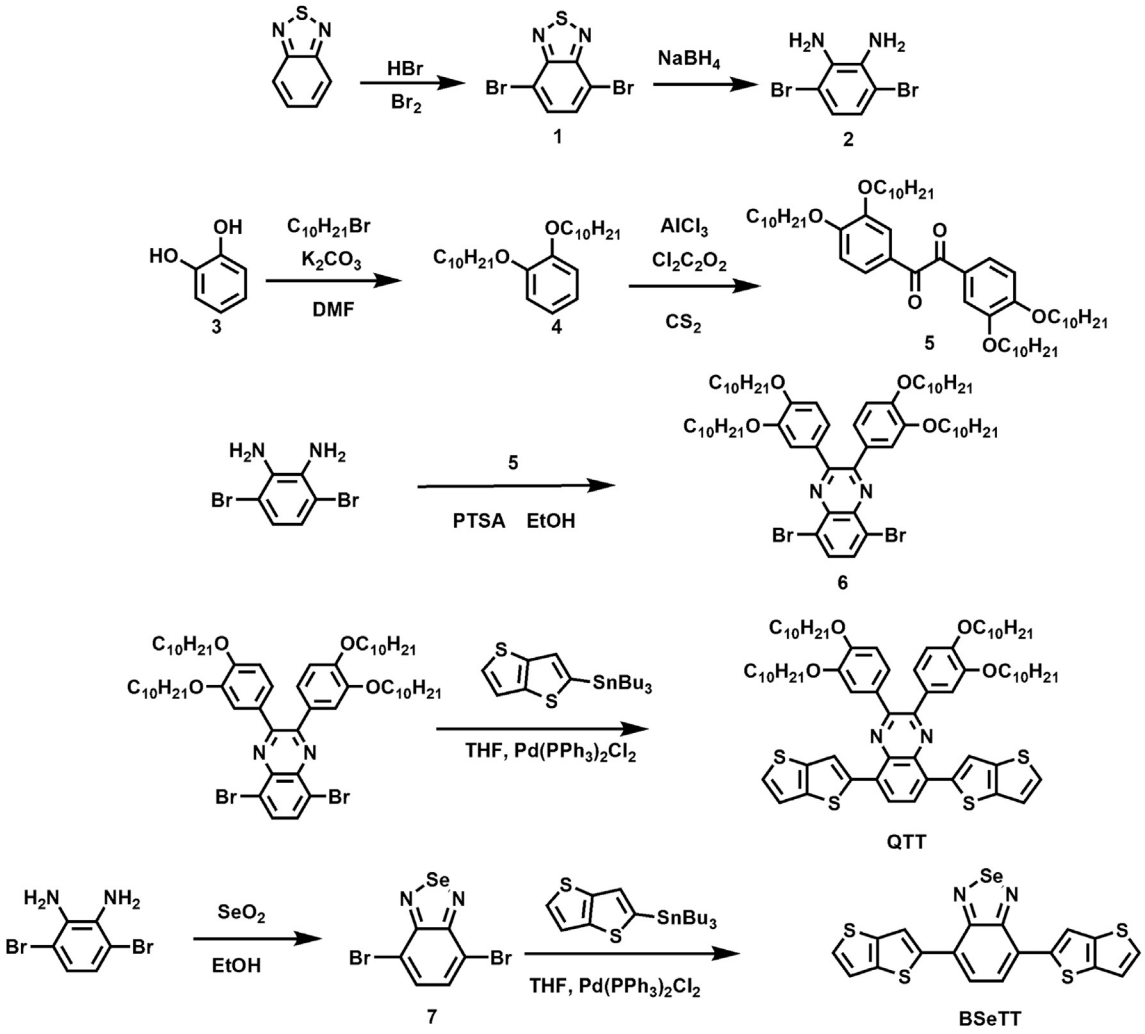

Scheme 1. Synthetic pathway for monomers.

Then, after each successive cycle formation of new reversible redox couples with an increasing current intensity were observed which prove the deposition of electroactive polymer films on ITO surface. (Fig. 1) After electrochemical polymerization, polymer coated ITO electrodes were subjected to CV in a monomer free 0.1 M $LiClO_4$/$NaClO_4$/ACN solution to investigate the redox behaviors of **PBSeTT** and **PQTT**. As illustrated in Fig. 2, reversible p-doping processes at 1.17 V for **PBSeTT** and at 0.7 V for **PQTT** were recorded.

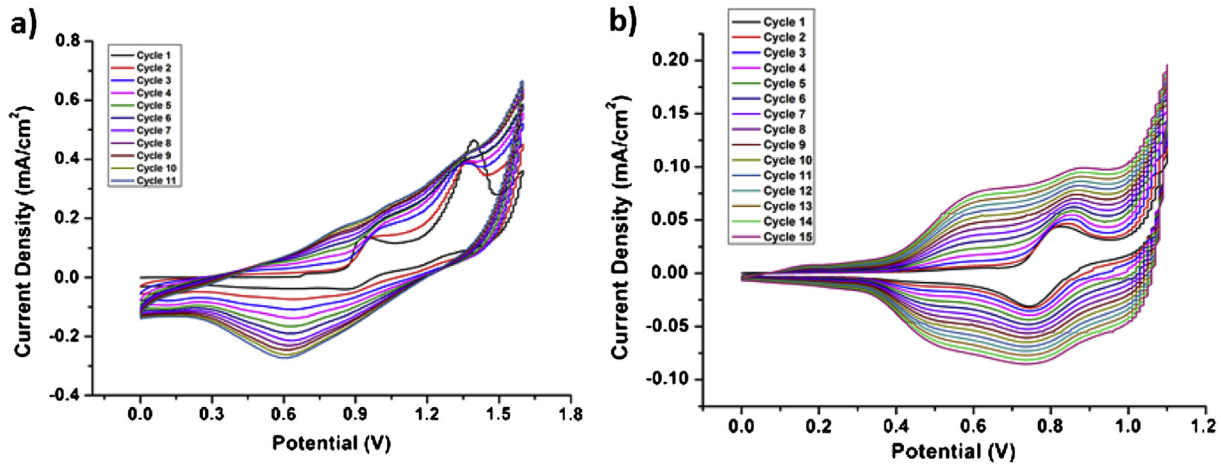

Fig. 1. Repeated potential scan electropolymerization of a) **BSeTT** in 0.1 M $NaClO_4$/$LiClO_4$ (1:1)/ACN:DCM (95:5) and b) **QTT** in 0.1 M $NaClO_4$/$LiClO_4$ (1:1)/ACN:DCM (1:1) on an ITO electrode at a scan rate of 100 mV/s.

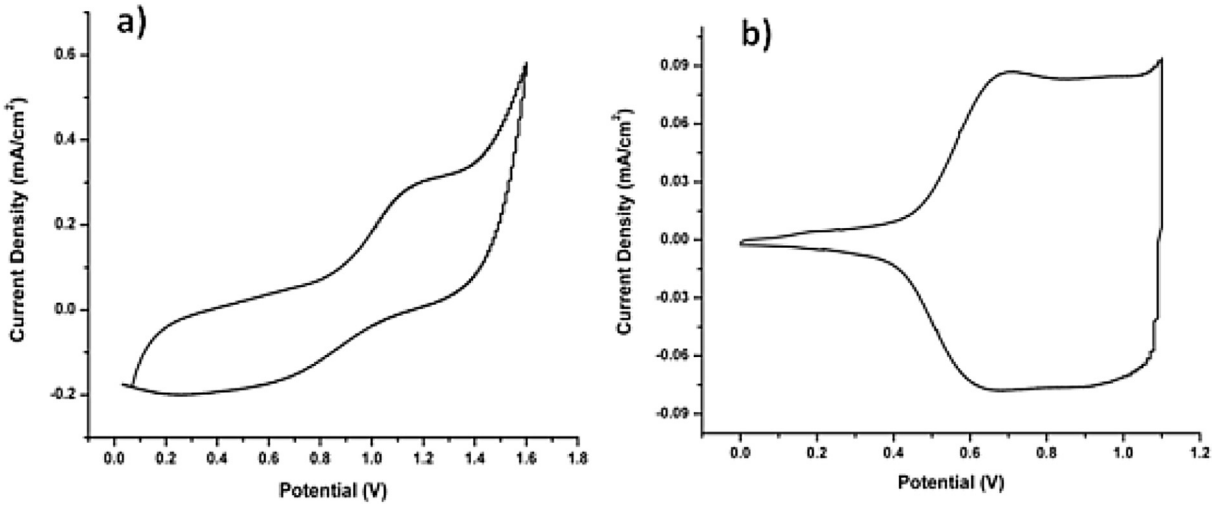

Fig. 2. Single scan cyclic voltammograms of electrochemically synthesized polymers a) **PBSeTT** and (b) **PQTT** in 0.1 M $LiClO_4/NaClO_4$ (1:1)/ACN solution.

When the shapes of single scan cyclic voltammograms are compared, it can be predicted that **PQTT** has a more charge trapping capacity than that of **PBSeTT**. In addition, in terms of the oxidation potentials of **PBSeTT** and **PQTT**, the lower oxidation potential of **PQTT** can be attributed to the different electron density of acceptor units in the structure. When benzoselenathiazole and quinoxaline derivatives were compared with previous examples, lower oxidation potentials of latter easily observed (Fig. 2), which is consistent with the literature.

HOMO–LUMO energy levels of conducting polymers are very important for their application areas and should be discussed. Using the onset of the corresponding oxidation potentials (Fig. 2)

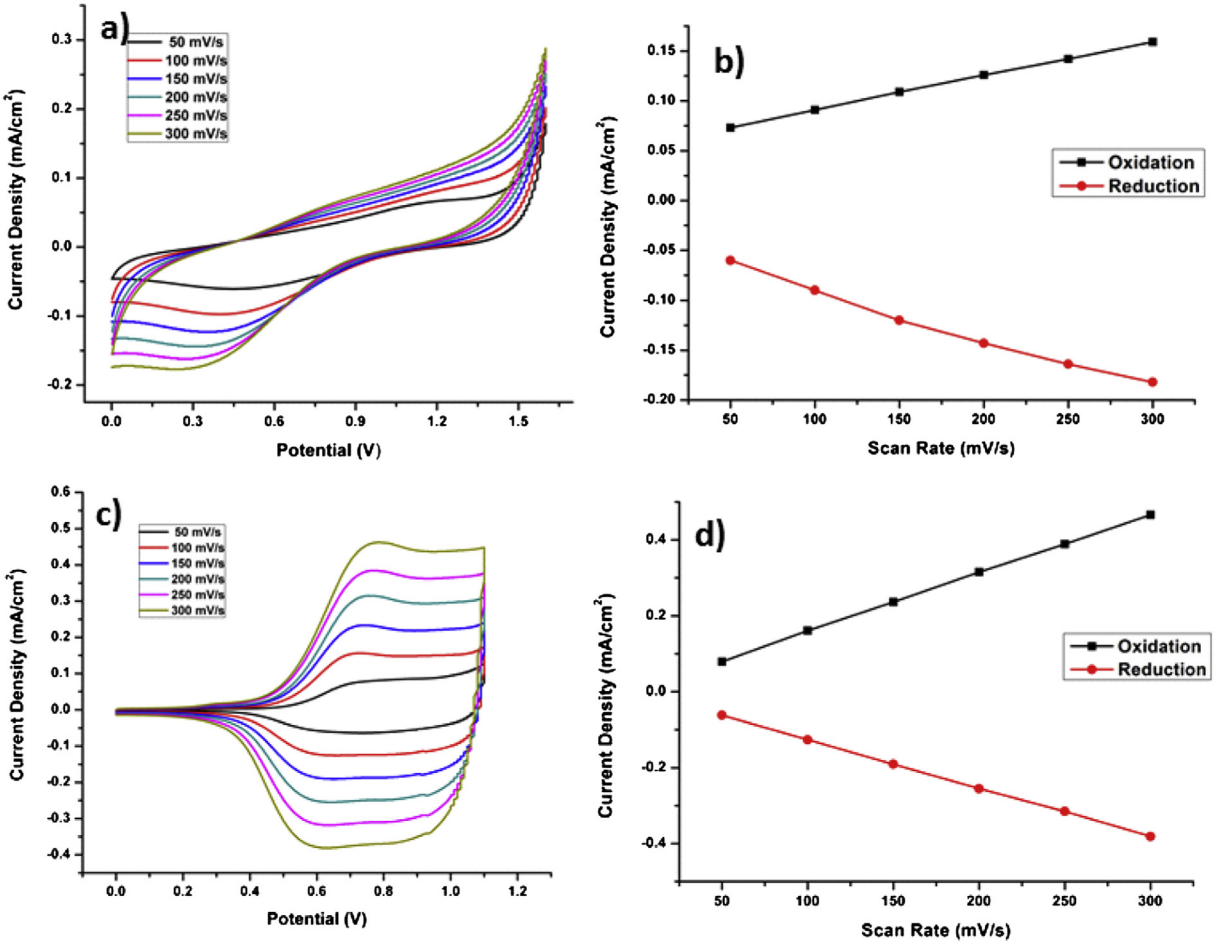

Fig. 3. Scan rate dependence of (a,b) **PBSeTT** and (c,d) **PQTT** in a 0.1 M $NaClO_4$–$LiClO_4$ (1:1)/ACN solution.

Table 1
Electrochemical and optical properties of **PBSeTT** and **PQTT**.

	HOMO(eV)	LUMO[a] (eV)	λ_{max} (nm)	E_g (eV)
PBSeTT	−5.88	−4.95	530	0.93
PQTT	−5.47	−4.17	442/600	1.30

[a] LUMO energy levels calculated using optical band-gap values and HOMO energy levels.

against Fc/Fc^+ reference electrode (NHE was taken as 4.75 eV vs. vacuum) HOMO energy levels were calculated as −5.88 eV and −5.47 eV for **PBSeTT** and **PQTT**. As mentioned before these polymers have only p-doping characteristics, hence LUMO energy levels were calculated using HOMO energy and optical band gap values and found as −4.95 eV and −4.17 eV, respectively.

The scan rate dependence of doping–dedoping processes is important to investigate whether this process is non-diffusion controlled or not. For this purpose single scan cyclic voltammograms of both polymer films were recorded at different scan rates and the scan rate dependence of both **PBSeTT** and **PQTT** (Fig. 3) were investigated. Linear relationship between the current density and the scan rate proves that the electroactive polymer films were well adhered and the redox processes were non-diffusion controlled. Results of electrochemical studies were reported in Table 1.

In the light of the points mentioned in this part, it can be clearly pointed out that both electrochemically synthesized polymers have only p-type doping character.

3.3. Spectroelectrochemical studies

Spectroelectrochemical studies mainly focus on optical changes and electronic transitions as a result of applied potentials. For these studies polymer films were prepared via electrochemically as described before and all these studies were conducted in 0.1 M $NaClO_4$–$LiClO_4$/ACN using UV–Vis–NIR spectrophotometer via incrementally increasing applied potential between 0.0 V and 0.95 V for **PBSeTT**, 0.0 V and 1.2 V for **PQTT** as decided from CV results reported in Fig. 2.

Before performing stepwise oxidation, both polymers (**PBSeTT** and **PQTT**) were reduced to their neutral states to get a real neutral state absorption and to remove any trapped charge and dopant ion remained from electrochemical polymerization. Upon stepwise oxidation, while the absorption in the visible region centered at 530 nm for **PBSeTT** started to decrease, new bands were appeared at around 900 nm and 1300 nm due to the formation of charge carriers on the polymer backbone namely polarons (radical cation) and bipolarons (dication) (Fig. 4a). While **PBSeTT** revealed only one absorption maxima in the visible region, two absorption maxima were recorded for **PQTT** centered at 442 nm and 600 nm which is similar to its quinoxaline based counterparts. Similar to **PBSeTT**, successive oxidation resulted in a decrease in neutral state absorptions with the formation of new bands at around 800 nm and 1200 nm for **PQTT**(Fig. 4b). Polymer **PQTT** could not be fully undoped since at negative voltages leakage of the film occurs from the electrode surface. From spectroelectrochemical studies, besides λ_{max} values, optical band gaps of these type of materials could be calculated which is a crucial parameter for their applications in different fields such as organic solar cells. Optical band gaps (Eg^{op}) of both polymer films were determined from the lowest energy π–π^* transitions (530 nm and 600 nm for **PBSeTT** and **PQTT**), and the following values were found as 0.93 eV and 1.30 eV respectively (Table 1). Calculated Eg^{op} values state that both polymers can be regarded as a low band gap polymers. While Fig. 4 reveals spectroelectrochemistry results of polymers, corresponding colors at the neutral and oxidized states were reported in Fig. 5.

From Figs. 4 and 5 it can be clearly pointed out that spectroelectrochemical studies are also consistent with the colors of polymer films in their neutral and oxidized states. Both polymers revealed different colors in their neutral and oxidized states. As seen in Fig 4, **PBSeTT** has a wide range of absorption (nearly full visible absorption) in the visible region which makes it dark gray in both states. Similar to other quinoxaline bearing donor–acceptor–donor type polymers two absorption peaks in the red (in the web version) and blue (in the web version) regions of the visible spectrum resulted in a neutral state green (in the web version) polymer, **PQTT**. After stepwise oxidation, **PQTT** revealed a gray colored oxidized state where almost all visible light was harvested by the polymer film.

3.4. Electrochromic contrast and switching studies

Both percent transmittance and switching times are crucial parameters for electrochromic materials. Switching time can be defined as the time required for the color change of a polymer between two extreme states (neutral and oxidized/reduced states). How fast the electrochromic materials change their colors affects the switching time. Percent transmittance values and switching

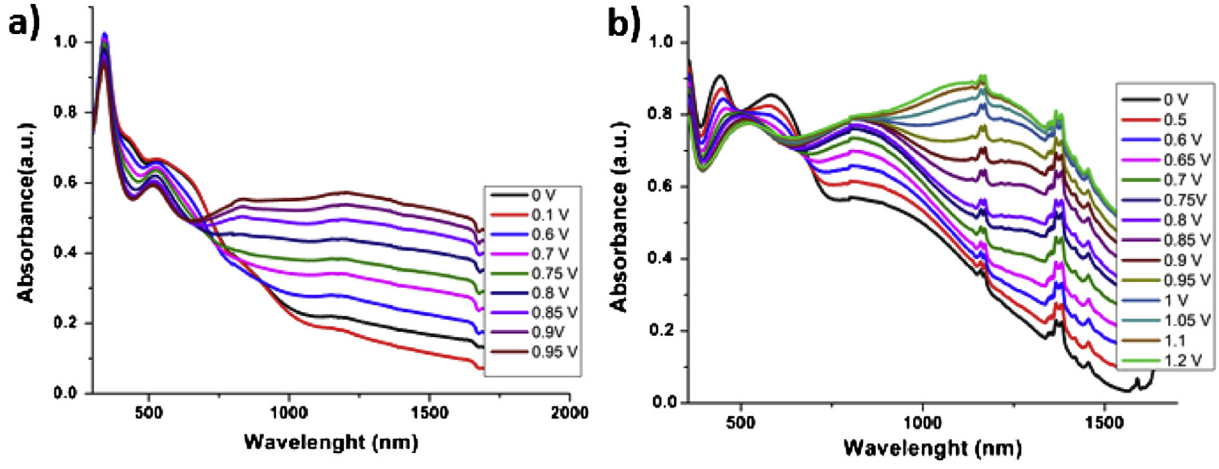

Fig. 4. Electronic absorption spectra of a) **PBSeTT** switching between 0.0 V and 0.95 V, b) **PQTT** between 0.0 V and 1.2 V in 0.1 M $NaClO_4$/$LiClO_4$(1:1)/ACN solution.

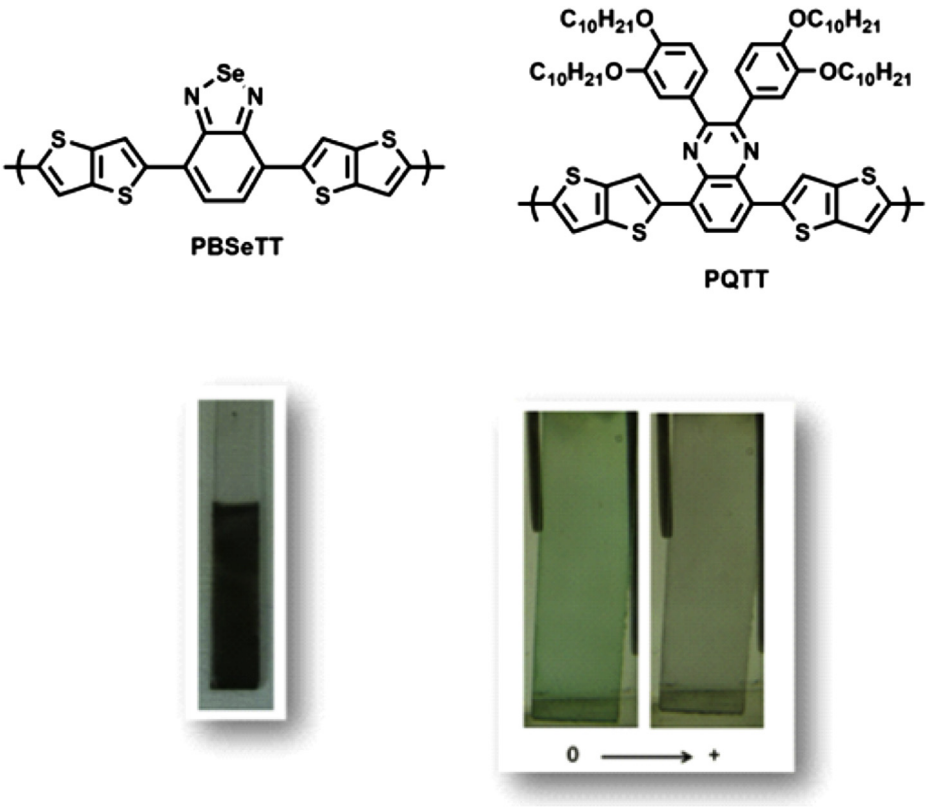

Fig. 5. Structures and colors of the polymers at neutral and oxidized states.

times for both polymers were monitored in visible and NIR regions by applying square-wave potential steps. Results were calculated from Fig. 6 and summarized in Table 2.

In this study two different groups (benzoselenathiazole and quinoxaline) were chosen as the acceptor units and coupled with fused donor unit, thieno[3,2-b]thiophene. The optical contrasts were observed for **PQTT** as 13% at 440 nm, 12% at 800 nm and 34% at 1180 nm with low switching times as 0.3 s, 0.3 s and 0.5 s respectively. Although the optical contrasts are not so high, the polymer film was stable upon repetitive cycles. **PBSeTT** revealed 13% optical contrast upon doping/de-doping processes with a switching time of 3.1 s in NIR region. It showed 4% optical contrast at 525 nm and 13% at 830 nm with 3.1 s and 1.4 s switching times at corresponding wavelengths.(Table 3)

When benzoselenathiazole and quinoxaline based polymers **PBSeTT** and **PQTT** are compared in terms of their electrochromic contrast and switching abilities, it was clearly seen that **PQTT** has shorter switching times and higher percent transmittance values than that of **PBSeTT** which is also consistent with the literature.

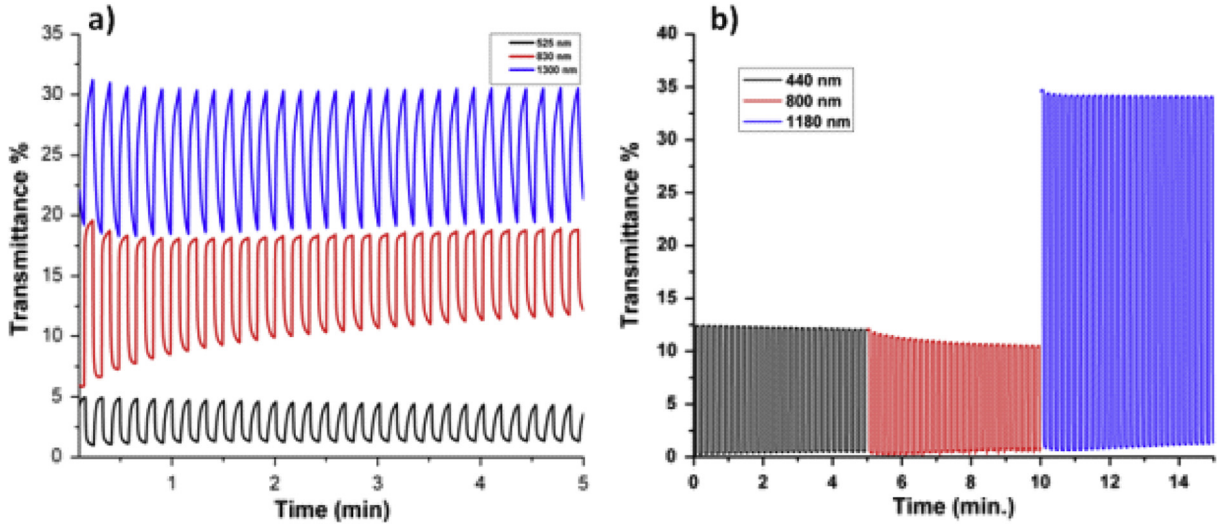

Fig. 6. Optical contrasts and switching times for (a) **PBSeTT** and (b) **PQTT** recorded at different wavelengths in 0.1 M $NaClO_4/LiClO_4$ (1:1)/ACN solution.

Table 2
Summary of kinetic and optic studies of **PBSeTT** and **PQTT**.

Optical contrast (ΔT%)			Switching time (s)
PBSeTT	4%	525 nm	3.1
	13%	830 nm	1.4
	13%	1300 nm	3.1
PQTT	13%	440 nm	0.3
	12%	800 nm	0.3
	34%	1180 nm	0.5

Table 3
Comparison of electrochemical and/or optical data for PBSeTT PQTT and previously synthesized polymers.

Polymers	Eox m [V]	Eox p [V]	λ_{max},1 [nm]	λ_{max},2 [nm]	λ_{max},3 [nm]	E_g [eV]
PBSeTT	1.39	1.13	525	–	–	0.93
PQTT	0.83	0.69	442	600	–	1.3
PTRzTT[a]	1.25	0.96	500	–	–	1.87
PESeE[a]	0.85	−0.09	343	448	796	1.05
PDOPEQ[a]	0.8	0.5	415	690	–	1.45

[a] References [33–35].

4. Conclusion

Two novel donor–acceptor–donor type monomers comprising benzoselenadiazole and quinoxaline units as the acceptor and thieno[3,2-b]thiophene as the donor group were successfully synthesized by Stille Coupling reaction (BSeTT and QTT). After the characterization of monomers, polymerizations were carried out electrochemically on ITO coated glass slides to examine their electrochemical and optical properties. Both polymers revealed different colors in their neutral and oxidized states. **PBSeTT** has a wide range of absorption (nearly full visible absorption) in the visible region which makes it dark gray in both states. Similar to other quinoxaline bearing donor–acceptor–donor type polymers two absorption peaks in the red and blue regions of the visible spectrum resulted in a neutral state green polymer, **PQTT**. After stepwise oxidation, **PQTT** revealed a gray colored oxidized state where almost all visible light was harvested by the polymer film. The band gap of the polymers were calculated to be 0.93 eV and 1.3 eV for PBSeTT and PQTT which is a proper value keeping in mind that polymers with DA units in general demonstrate band gaps between 0.9 eV and 1.3 eV. Comparison among monomers showed that increasing electron density of donor units decreases the band gap of the monomers where donor–acceptor couple is a substantial effect on the electronic properties of donor–acceptor–donor material. **PQTT** has lower oxidation potential and band gap. **PQTT** will be used as active materials in future display technology. Moreover, **PBSeTT** which has broadest absorption than others which makes it a good candidate for solar cell applications.

References

[1] Shirakawa H, Louis EJ, MacDiarmid AG, Chinag CK, Heeger A. J Chem Commun 1977;16:578–80.
[2] Yu G, Gao J, Hummelen JC, Wudl F, Heeger A. Science 1995;270:1789–91.
[3] Kim JY, Lee K, Coates NE, Moses D, Nguyen TQ, Dante M, et al. Science 2007;317:222–5.
[4] Zou Y, Najari A, Berrouard P, Beaupre S, Aich RB, Tao Y, et al. J Am Chem Soc 2010;132:5330–1.
[5] Su H, Wu F, Shu C, Tung Y, Yun C, Lee G. J Polym Sci Part A Polym Chem 2005;43:859–69.
[6] Tsai JH, Chueh CC, Chen WC, Yu CY, Hwang GW, Ting C, et al. J Polym Sci Part A Polym Chem 2010;48:1669–75.
[7] Hongmei X, Kai Z, Chunhui D, Shengjian L, Fei H, Yong C. Polymer 2012;53:5675–83.
[8] Ting L, Yue C, Yunlong F, Chen-Jiang L, Si-Chun Y, Jian P. J Am Chem Soc 2011;133(16):6099–101.
[9] McQuede DT, Pullen AE, Swager TM. Chem Rew 2000;100:2537–74.
[10] Roncali J. Chem Rew 1997;97:173–206.
[11] Roncali J. J Mater Chem 1999;9:1875–93.
[12] Chu TY, Alem S, Tsang SW, Tse SC, Wakim S, Lu JP, et al. Appl Phys Lett 2011;98:253–301.
[13] He Z, Zhong C, Huang X, Wong W, wu H, Chen L, et al. Adv Mater 2011;23:4636–43.
[14] Hou JH, Chen HY, Zhang SQ, Chen RI, Yang Y, Wu Y, et al. J Am Chem Soc 2009;131:15586–7.
[15] Balan A, Baran D, Gunbas G, Durmus A, Ozyurt F, Toppare L. Chem Commun; 2009:6768–70.
[16] Xiao P, Hong W, Li Y, Dumur Y, Graff B, Fouassier JP, et al. Polymer 2014;55:746–51.
[17] Zoombelt AP, Leenen MAM, Fonrodona M, Nicolas Y, Wienk MM, Janssen RAJ. Polymer 2009;50:4564–70.
[18] Sakthivel P, Song HS, Chakravarthi N, Lee JW, Gal YS, Hwang S, et al. Polymer 2013;54:4883–93.
[19] Boudreault PT, Michaud A, Leclerc M. Macro Rap Commun 2007;28:2176–9.
[20] (a) Hou Q, Xu Y, Yang W, Yuan M, Peng J, Cao Y. J Mater Chem 2002;12:2887–92;
(b) Zhang S, Guo Y, Fan H, Liu Y, Chen HY, Yang G, et al. J Polym Sci Part A Polym Chem 2009;47:5498–508;
(c) Mei J, Heston NC, Vasilyeva SV, Reynolds JR. Macromolecules 2009;42:1482–7.
[21] Blouin N, Michaud A, Gendron D, Wakim S, Blair E, Neagu-Plesu R, et al. J Am Chem Soc 2008;130:732–42.
[22] Hou J, Park MH, Zhang S, Yao Y, Chen LM, Li JH, et al. Macromolecules 2008;41:6012–8.
[23] Qin R, Li W, Li C, Du C, Veit C, Schleiermacher HF, et al. Am Chem Soc 2009;131:14612–3.
[24] Huo L, Hou J, Zhang S, Chen HY, Yang Y. Angew Chem Int Ed 2010;49:1500–3.
[25] Patra A, Wijsboom YH, Zade SS, Li M, Sheynin Y, Leitus G, et al. J Am Chem Soc 2008;130:6734–6.
[26] Lee Y, Nam YM, Jo WH. J Mater Chem 2011;21:8583–90.
[27] (a) Bredas JL, Norton JE, Cornil J, Coropceanu V. Acc Chem Res 2009;42:1691–9;
(b) Liu Y, Liu Y, Zhan X. Macrom Chem Phys 2011;212:428–43;
(c) Wu JS, Lin CT, Wang CL, Cheng YJ, Hsu CS. Chem Mater 2012;24:2391–9;
(d) Kim JH, Kim HU, Kang IN, Lee SK, Moon SJ, Shin WS, et al. Macromolecules 2012;45:8628–38.
[28] (a) Ajayaghosh A. Chem Soc Rev 2003;32:181–91;
(b) Jung IH, Jung YK, Lee J, Park J-H, Woo HY, Lee J-I, et al. J Polym Sci Part A Polym Chem 2008;46:7148–61.
[29] (a) Chen M, Perzon E, Andersson MR, Marcinkevicius S, Jönsson SKM, Fahlman M, et al. Appl Phys Lett 2004;84:3570–2;
(b) Raimundo JM, Blanchard P, Brisset H, Akoudad S, Roncali J. J Chem Commun; 2000:939–40.
[30] Tsubata Y, Suzuki T, Hiyashi T, Yamashita Y. J Org Chem 1992;57:6749–55.
[31] Zhu SS, Swager TM. J Am Chem Soc 1997;119:12568–77.
[32] Bird CW, Chseesman WH, Sarefield AA. J Chem Soc 1968;90:4767–70.
[33] Gunbas G, Durmus A, Toppare L. Adv Funct Mater 2008;18:2026–30.
[34] Akbasoglu N, Balan A, Baran D, Cirpan A, Toppare L. J Polym Sci Part A Polym Chem 2010;48:5603–10.
[35] Cihaner A, Algı F. Adv Funct Mater 2008;18:3583–9.